Hydrometalation of P≡CBu^t and Activation of the P−C Bond by a Tetrairidium Carbonyl Cluster: Solution Characterization of [Ir$_4$Pt(dppe)(CO)$_n${μ-PC(H)Bu^t}(μ-PPh$_2$)] (n = 10 and 9) and Crystal and Molecular Structures of the Phosphinidine Complex [HIr$_4$Pt(dppe)(μ-CO)(CO)$_7$(μ-PCH$_2$Bu^t)(μ-PPh$_2$)] and of the Partially Encapsulated Phosphide Compound [Ir$_4$Pt(dppe)(μ-CO)(CO)$_8$(μ_5-P)(μ-PPh$_2$)]

Maria Helena Araujo,[†] Anthony G. Avent,[†] Peter B. Hitchcock,[†] John F. Nixon,*[,†] and Maria D. Vargas*[,‡]

School of Chemistry, Physics and Environmental Science, University of Sussex, Brighton, BN1 9QJ, U.K., and Instituto de Química, Universidade Estadual de Campinas, CP 6154, Campinas, 13083-970, SP, Brazil

Received April 24, 1998

Reaction of [HIr$_4$(CO)$_{10}$(μ-PPh$_2$)], **1**, with [Pt(dppe)(η^2-PCBu^t)] yields four Ir$_4$Pt clusters [Ir$_4$Pt(dppe)(CO)$_n${μ-PC(H)Bu^t}(μ-PPh$_2$)] (n = 10, **2**, and 9, **3**), [HIr$_4$Pt(dppe)(μ-CO)(CO)$_7$(μ-PCH$_2$Bu^t)(μ-PPh$_2$)], **4**, and [Ir$_4$Pt(dppe)(μ-CO)(CO)$_8$(μ_5-P)(μ-PPh$_2$)], **5**. These compounds contain fragments arising from hydrometalation and cleavage of the P−C triple bond of the phosphaalkyne. The structures of compounds **2** and **3**, isolated as a mixture, were proposed on the basis of multinuclear NMR and mass spectrometry. To our knowledge these are the first examples of clusters containing a phosphido fragment {μ-PC(H)Bu^t} originating from hydrometalation of the phosphaalkyne. Compounds **4** and **5** were characterized in solution by multinuclear NMR spectroscopy, and their solid-state structures were determined by X-ray analyses. A remarkably low $^1J_{P-Pt}$ coupling constant in the Pt(dppe) fragment of the former square-based pyramidal compound is discussed.

Introduction

There is current interest in comparative studies of the coordination chemistry of phosphaalkynes and alkynes.[1] In contrast with the large number of carbonyl clusters reported to react with alkynes,[2] [HM$_3$(CO)$_9$(μ_3-η^2-PCBu^t)]$^-$ (M = Fe, Ru)[3] are the only examples of cluster compounds resulting from ligand substitution with PCBu^t. The compound [HIr$_4$(CO)$_{10}$(μ-PPh$_2$)], **1**, reacts with phosphines L to give [HIr$_4$(CO)$_{10-n}$L$_n$(μ-PPh$_2$)] (n = 1−3),[4] but no reaction occurs with PCBu^t or with alkynes,[5] although [HIr$_4$(CO)$_9$(Ph$_2$PC≡CPh)(μ-PPh$_2$)] reacts with PCBu^t to give [Ir$_4$(CO)$_8${μ_4-η^3-Ph$_2$PC(H)C(Ph)PCBu^t}(μ-PPh$_2$)], as a result of an alkyne−phosphaalkyne coupling and incorporation of the cluster-bound H atom.[6] It is known that once PCBu^t is π-coordinated, the phosphorus lone electron pair becomes available for further coordination, and considering that [Pt(dppe)(η^2-PCBu^t)][7] exhibits enhanced reactivity toward metal centers,[8] we attempted to use it as a PCBu^t transfer reagent toward cluster **1**. We now describe four novel Ir$_4$Pt clusters resulting from (i) insertion of coordinated PCBu^t into the Ir−H−Ir bond of **1** and (ii) P−C bond activation of coordinated PCBu^t ligands. Hydrometalation of phosphaalkynes has only been recently reported in mononuclear Ru and Zr systems.[9,10]

Experimental Section

General Procedures. All manipulations and reactions were conducted under argon, unless otherwise specified, using

[†] University of Sussex.
[‡] Universidade Estadual de Campinas.

(1) Nixon, J. F. *Coord. Chem. Rev.* **1995**, *145*, 201, and references therein.
(2) Sappa, E.; Tiripicchio, A.; Braunstein, P. *Chem. Rev.* **1983**, *83*, 3.
(3) Meidine, M. F.; Nixon, J. F.; Mathieu, R. *J. Organomet. Chem.* **1986**, *314*, 307.
(4) (a) Livotto, F. S.; Raithby, P.; Vargas, M. D. *J. Chem. Soc., Dalton Trans.* **1993**, 1797. (b) Ziglio, C. M.; Vargas, M. D.; Braga, D.; Grepioni, F. Unpublished results.
(5) Araujo, M. H. Ph.D. Thesis, Universidade Estadual de Campinas, Brazil, 1995.
(6) Benvenutti, M. H. A.; Hitchcock, P. B.; Nixon, J. F.; Vargas, M. D. *J. Chem. Soc., Chem. Commun.* **1994**, 1869.
(7) Al-Resayes, S. I.; Hitchcock, P. B.; Meidine, M. F.; Nixon, J. F. *J. Chem. Soc., Chem. Commun.* **1984**, 1080.
(8) (a) Bartsch, R.; Hitchcock, P. B.; Meidine, M. F.; Nixon, J. F. *J. Organomet. Chem.* **1984**, *266*, C41. (b) Meidine, M. F.; Meir, C. J.; Morton, S.; Nixon, J. F. *J. Organomet. Chem.* **1985**, *297*, 255.
(9) (a) Bedford, R. B.; Hibbs, D. E.; Hill, A. F.; Hursthouse, M. B.; Abdul Malik, K. M.; Jones, C. *J. Chem. Soc., Chem. Commun.* **1996**, 1895. (b) Bedford, R. B.; Hill, A. F.; Jones, C.; White, A. J. P.; Wilton-Ely, J. D. E. T. *J. Chem. Soc., Dalton Trans.* **1997**, 139.
(10) Benvenutti, M. H. A.; Cenac, N.; Nixon, J. F. *Chem. Commun.* **1997**, 1327.

10.1021/om980317w CCC: $15.00
Publication on Web 11/07/1998

standard Schlenk techniques. CH_2Cl_2 was dried over CaH_2, and hexane over sodium wire. Solvents were freshly distilled under N_2 from Na/K alloy (hexane) or from CaH_2 (CH_2Cl_2) prior to use. $[HIr_4(CO)_{10}(\mu\text{-}PPh_2)]$,[4] **1**, and $[Pt(dppe)(\eta^2\text{-}PCBu^t)]$[7] were prepared by literature methods.

Preparative TLC was carried out in air by using ca. 2 mm thick glass-backed silica plates (20 × 20 cm) prepared from silica gel type GF_{254} (Fluka) and CH_2Cl_2−hexane (3:7) as eluent, and the compounds were extracted from silica with CH_2Cl_2.

IR spectra were obtained on a 1600 Perkin-Elmer spectrometer scanning between 2200 and 1600 cm^{-1}, using CaF_2 cells. Microanalyses were performed on a CEC 240XA analyzer by Medac Ltd., U.K. Routine ^1H (300.0 MHz), ^{13}C (75.43 MHz), and ^{31}P (121.44 MHz) NMR spectra were recorded with a Bruker DPX 300. Chemical shifts are given in ppm using deuterated solvents as lock and reference (^1H and $^{13}C\{^1H\}$, $SiMe_4$; $^{31}P\{^1H\}$ 85% H_3PO_4, (external); ^{195}Pt, Na_2PtCl_6 (external, δ 0 in D_2O)); coupling constants (J) are given in hertz. The detailed NMR studies have been carried out using CD_2Cl_2 solutions and a Bruker AMX 500 spectrometer. Standard pulse sequences were used for the NMR experiments.[11] The ^{13}CO enriched samples (25−30%) were prepared starting from $Bu_4N[Ir_4(CO)_{11}Br]$.[12] Electrospray mass spectra (ESMS) were obtained in positive-ion mode with a VG Platform II mass spectrometer using MeOH as the mobile phase at the University of Waikaito, New Zealand. A solution of the metal carbonyl was prepared in MeOH (ca. 1 mL), and one drop of F_3CCOOH, or of a solution of $AgNO_3$ or $AgClO_4$, was added. The samples were injected via a Rheodyne injector fitted with a 10 μL sample loop and delivered to the spectrometer source (60 °C) at 0.01 cm^3 min^{-1}. Nitrogen was used as the drying and nebulizing gas. Cone voltages were varied from 20 to 50 V.[13]

Reaction of 1 with $[Pt(dppe)(\eta^2\text{-}PCBu^t)]$. To a solid mixture of **1** (0.30 g, 0.24 mmol) and $[Pt(dppe)(\eta^2\text{-}PCBu^t)]$ (0.17 g, 0.24 mmol) was added 15 mL of CH_2Cl_2, and the resulting solution was left stirring at room temperature. After ca. 10 min the color began to change from orange to dark green. Depending on the reaction time, three or four products were identified in the reaction mixture by $^{31}P\{^1H\}$ NMR measurements and isolated after separation by TLC: (i**)** after 4 h, compounds **2** (10%) and **3** (40%) were obtained as an orange mixture and compounds **5** (brown, 30%) and **1** (orange, 20%) as pure crystalline solids, (ii**)** after 5 days, four compounds were obtained, **2** (40%) and **3** (40%) as an orange mixture and **4** (red, 5%) and **5** (10%) as pure crystalline solids.

Characterization of Compounds $[Ir_4Pt(dppe)(CO)_{10}\{\mu\text{-}PC(H)Bu^t\}(\mu\text{-}PPh_2)]$, 2 and $[Ir_4Pt(dppe)(CO)_9\{\mu\text{-}PC(H)Bu^t\}(\mu\text{-}PPh_2)]$, 3, Isolated as a Mixture. IR ν_{CO} (CH_2Cl_2) for **2** and **3**: 2086 m, 2060 s, 2011 vs, and 1965 vs cm^{-1}. ESMS (MeOH/H^+ cone voltage = 20 V): for **2** *m*/*z* 1931 (100) and for **3** *m*/*z* 1903 (45). NMR (CD_2Cl_2, 25 °C): ^1H for **2**, δ 4.2 (dd, CH, J_{H-P} 12 and 3 Hz), 0.5 (s, 9H, CMe_3); for **3**, δ 1.3 (s, 9H, CMe_3) 5.2 (d, CH, J_{H-P} 3 Hz); for **2** and **3**, δ 1.5−1.8 and 1.9−2.6 (m, $Ph_2PCH_2CH_2PPh_2$), 7.9−6.5 (m, C_6H_5). $^{31}P\{^1H\}$: for **2**, δ 211.6 ($P_{1'}$) (ddd, $J_{P1'-P3'}$ 273, $J_{P1'-P4'}$ 161, $J_{P1'-P2'}$ 15, $J_{P1'-Pt}$ 2086 Hz), 51.0 ($P_{2'}$) (dd, $J_{P2'-P3'}$ 10, $J_{P2'-Pt}$ 3733 Hz), 45.6 ($P_{3'}$) (ddd, $J_{P3'-P4'}$ 9, $J_{P3'-Pt}$ 2592 Hz), − 81.8 ($P_{4'}$) (dd, $J_{P4'-Pt}$ 162 Hz); for **3**, δ 187.1 (P_1) (dd, J_{P1-P4} 154, J_{P1-P2} 11 Hz), 52.0 (P_2) (dd, J_{P2-P4} 10, J_{P2-Pt} 3322 Hz), 57.8 (P_3) (d, J_{P3-P4} 361, J_{P3-Pt} 2397 Hz), 145.4 (P_4) (ddd, J_{P4-Pt} 2038 Hz). $^{13}C\{^1H\}$ (at 25 °C) for **2** and **3**: δ 30.9 (d, CCH_3, J_{P-C} 13 Hz), 30.2 (d, CCH_3, J_{P-C} 7 Hz), 31.7−29.3 (m, $Ph_2PCH_2CH_2PPh_2$), 33.3 (d, CCH_3, J_{P-C} 6 Hz), 39.1 (d, CCH_3, J_{P-C} 3 Hz), 37.5 (d, *C*H, J_{P-C} 7 Hz), 38.0 (d, *C*H, J_{P-C} 8 Hz), 133.7−127.3 (m, C_6H_5). $^{13}C\{^1H\}$ (^{13}CO at − 90 °C): 182.0 (2 CO), 180.0 (CO), 178.6 (CO), 177.1 (CO), 176.3 (CO), 175.0 (CO), 172.4 (3 CO), 170.0 (CO), 167.6 (2 CO), 166.0 (CO), 165.7 (CO), 163.0 (CO), 161.0 (CO), 159.2 (CO), and 155.0 (CO). $^{195}Pt\{^1H\}$ (107.49 MHz) (δ to high frequency of $\Xi(^{195}Pt)$ = 21.4 MHz): for **2**, δ 1126; and for **3**, δ 992.

Characterization of $[HIr_4Pt(dppe)(\mu\text{-}CO)(CO)_7(\mu\text{-}PCH_2Bu^t)(\mu\text{-}PPh_2)]$, 4. IR ν_{CO} (CH_2Cl_2): 2046 m, 2026 s, 2008 s and 1785 m cm^{-1}. Anal. Calcd for $C_{51}H_{46}O_8P_4PtIr_4\cdot CH_2Cl_2\cdot {}^1/_2C_6H_{14}$: C, 30.6; H, 2.3. Found: C, 30.3; H, 1.7. NMR (CD_2Cl_2, 25 °C): ^1H (500 MHz), δ −16.6 (m, 1H), 0.7 (s, 9H, $C(CH_3)_3$), 0.8 (m, 1H, PCH_2Bu^t), 1.9 (m, 1H, PCH_2Bu^t), 2.1 (m, 2H, $Ph_2PCH_2CH_2PPh_2$), 2.8 (m, 2H, $Ph_2PCH_2CH_2PPh_2$), and 6.8−8.5 (m, 30H, C_6H_5). $^{31}P\{^1H\}$ (202.40 MHz): δ 154.2 (P_1) (ddd, J_{P1-P3} 180, J_{P1-P4} 109, J_{P1-P2} 9, J_{P1-Pt} 637 Hz), 40.0 (P_2) (dd, J_{P2-P4} 38, J_{P2-Pt} 153 Hz), 34.5 (P_3) (d, J_{P3-Pt} 181 Hz), 101.8 (P_4) (dd, J_{P4-Pt} 107 Hz). $^{13}C\{^1H\}$ (125.72 MHz): δ 29.7 (d, CCH_3, J_{P-C} 9 Hz), 33.6 (s, CCH_3), 30.6 (m, $Ph_2PCH_2CH_2PPh_2$), 33.3 (m, $Ph_2PCH_2CH_2PPh_2$), 51.4 (m, PCH_2Bu^t), 133.2 (d, C_{quat}, J_{P-C} 48 Hz), 134.8 (d, C_{quat}, J_{P-C} 46 Hz), 139.1 (d, C_{quat}, J_{P-C} 42 Hz), 141.9 (d, C_{quat}, J_{P-C} 31 Hz), 136.2−127.4 (C_6H_5), 166.3 (*C*O), 170.7 (*C*O), 175.6 (*C*O), 180.4 (*C*O), 183.8 (*C*O), 191.8 (*C*O), 201.9 (*C*O), 221.7 (*C*O).

X-ray Crystal Structure Analysis of $4\cdot CH_2Cl_2\cdot {}^1/_2C_6H_{14}$. Crystal data for **4** are summarized in Table 2. The compound, obtained as red crystals by slow diffusion of hexane in a very concentrated solution of **4** in CH_2Cl_2, crystallizes in the monoclinic space group $P2_1/c$. Data collection in the range $2° < \theta < 20°$ was performed using ω scans on an Enraf-Nonius CAD-4 diffractometer using Mo Kα radiation. From 5818 measured reflections, all 5630 independent reflections were used, and 352 parameters were refined by full-matrix least-squares against all F^2 data (SHELXL-93);[14] Ir, Pt, Cl, and P atoms were anisotropic. Owing to limited data, the C and O atoms were left isotropic. H atoms were included in riding mode with U_{iso}(H) equal to $1.2U_{eq}$(C) or $1.5U_{eq}$(C) for methyl groups. The hydride H atom was omitted. Loose distance constraints were applied to the solvate molecules. The structure was solved using direct methods (SHELXL-86).[14] The refinement converged with R1 = 0.065 [for 3414 reflections with $I > 2\sigma(I)$], wR2 = 0.173 (all data).

Characterization of $[Ir_4Pt(dppe)(\mu\text{-}CO)(CO)_8(\mu_5\text{-}P)(\mu\text{-}PPh_2)]$, 5. IR ν_{CO} (CH_2Cl_2): 2034 vs, 1900 m, 1896 s, and 1843 sh cm^{-1}. Anal. Calcd for $C_{47}H_{34}O_9P_4PtIr_4\cdot 2CH_2Cl_2$: C, 28.2; H, 1.7. Found: C, 27.7; H, 1.3. NMR ($CDCl_3$, 25 °C): ^1H, δ 1.6−2.5 (m, 4H, $Ph_2PCH_2CH_2PPh_2$), 8.1−6.7 (m, 30H, C_6H_5). $^{31}P\{^1H\}$: δ 283.1 (P_1) (ddd, J_{P1-P3} 319, J_{P1-P2} 58, J_{P1-P4} 7, J_{P1-Pt} 2575 Hz), 55.0 (P_2) (dd, J_{P2-P4} 58, J_{P2-P3} 5, J_{P2-Pt} 3256 Hz), 61.0 (P_3) (dd, J_{P3-Pt} 3296 Hz), 102.6 (P_4) (dd, J_{P4-Pt} 90 Hz). $^{13}C\{^1H\}$: δ 28.1 (m, $Ph_2PCH_2CH_2PPh_2$), 31.7 (m, $Ph_2PCH_2CH_2PPh_2$), 126.5−141.5 (m, C_6H_5).

X-ray Crystal Structure Analysis of $5\cdot 2CH_2Cl_2$. Crystal data for **5** are summarized in the Supporting Information. Compound **5** was obtained as brown crystals (bad quality crystals) by slow evaporation of a very concentrated solution in CH_2Cl_2.

Results and Discussion

The reaction between $[HIr_4(CO)_{10}(\mu\text{-}PPh_2)]$, **1**, and $[Pt(dppe)(\eta^2\text{-}PCBu^t)]$ in CH_2Cl_2, at 25 °C, was followed by $^{31}P\{^1H\}$ NMR. After 4 h three compounds were observed, **3** and **5** as major products and **2** as a minor

(11) Mann, B. E. *Adv. Organomet. Chem.* **1988**, *28*, 397, and references therein.

(12) Chini, P.; Ciani, G.; Garlaschelli, L.; Manassero, M.; Martinengo, S.; Sironi, A.; Canziani, F. *J. Organomet. Chem.* **1978**, *152*, C35,

(13) Nicholson, B. K. Department of Chemistry, University of Waikato, Hamilton, New Zealand.

(14) Enraf-Nonius CAD-4 Software, Version 5.0; Enraf-Nonius: The Netherlands, 1989. Sheldrick, G. M. SHELXS-86. Program for the Solution of Crystal Structures; University of Gottingen: Germany, 1985. Sheldrick, G. M. SHELXL-93. Program for Crystal Structure Refinement; University of Gottingen: Germany, 1993. Watkin, D. J.; Pearce, L. J. CAMERON. An Interactive Graphics Editor; University of Oxford: England, 1993.

Scheme 1

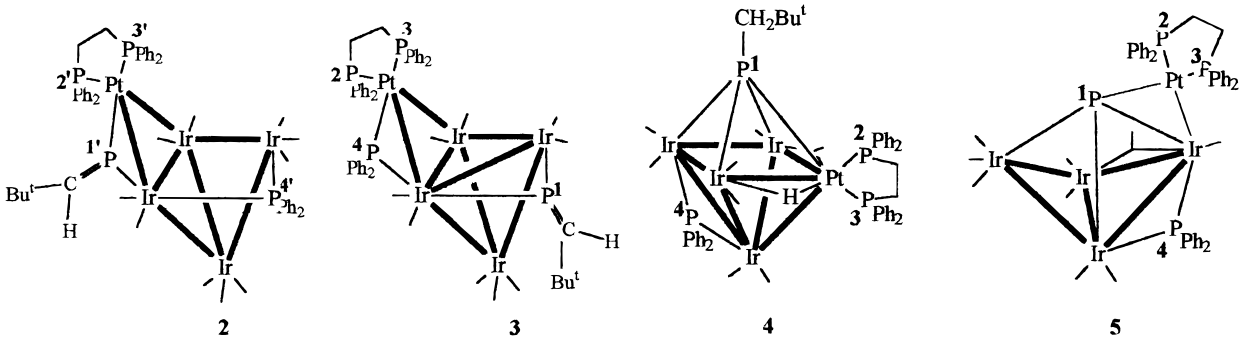

2 **3** **4** **5**

Table 1. $^{31}P\{^1H\}$ NMR Data for Compounds 2, 3, 4, and 5 in CD_2Cl_2 at 25 °C[a,b]

compound **2**		compound **3**		compound **4**		compound **5**	
δ	J_{P-P} and J_{P-Pt}	δ	J_{P-P} and J_{P-Pt}	δ	J_{P-P} and J_{P-Pt}	δ	J_{P-P} and J_{P-Pt}
$P_{1'}$ 211.6	$P_{1'}-P_{3'}$ 273	P_1 187.1	P_1-P_4 154	P_1 154.2	P_1-P_3 180	P_1 283.1	P_1-P_3 319
(ddd)	$P_{1'}-P_{4'}$ 161	(dd)	P_1-P_2 11	(ddd)	P_1-P_4 109	(ddd)	P_1-P_2 58
	$P_{1'}-P_{2'}$ 15				P_1-P_2 9		P_1-P_4 7
	$P_{1'}-Pt$ 2086				P_1-Pt 637		P_1-Pt 2575
$P_{2'}$ 51.0	$P_{2'}-P_{3'}$ 10	P_2 52.0	P_2-P_4 10	P_2 40.0	P_2-P_4 38	P_2 55.0	P_2-P_1 58
(dd)	$P_{2'}-P_{1'}$ 15	(dd)	P_2-P_1 11	(dd)	P_2-P_1 9	(dd)	P_2-P_4 58
	$P_{2'}-Pt$ 3733		P_2-Pt 3322		P_2-Pt 153		P_2-P_3 5
							P_2-Pt 3256
$P_{3'}$ 45.6	$P_{3'}-P_{1'}$ 273	P_3 57.8	P_3-P_4 361	P_3 34.5	P_3-P_1 180	P_3 61.0	P_3-P_1 319
(ddd)	$P_{3'}-P_{2'}$ 10	(d)	P_3-Pt 2397	(d)	P_3-Pt 181	(dd)	P_3-P_2 5
	$P_{3'}-P_{4'}$ 9						P_3-Pt 3296
	$P_{3'}-Pt$ 2592						
$P_{4'}$ −81.8	$P_{4'}-P_{1'}$ 161	P_4 154.4	P_4-P_3 361	P_4 101.8	P_4-P_1 109	P_4 102.6	P_4-P_2 58
(dd)	$P_{4'}-P_{3'}$ 9	(ddd)	P_4-P_1 154	(dd)	P_4-P_2 38	(dd)	P_4-P_1 7
	$P_{4'}-Pt$ 162		P_4-P_2 10		P_4-Pt 107		P_4-Pt 90
			P_4-Pt 2038				

[a] Chemical shifts in ppm, coupling constants in Hz. [b] Chemical shifts positive to high frequency of 85% H_3PO_4 (external).

product, besides some unreacted starting material. After 5 days no more starting material was detected, compounds **2** and **3** were the major products, and a new compound, **4**, was obtained in low yield. The concentration of **5** in the reaction mixture changed during the 5 day stirring, due to the instability of this compound in solution.

The major orange products **2** and **3** (ca. 40% each), which could not be separated by TLC or by fractional crystallization, were stable in hydrocarbon solvents under Ar but slowly decomposed in more polar solvents. They were formulated as $[Ir_4Pt(dppe)(CO)_{10}\{\mu\text{-PC(H)Bu}^t\}(\mu\text{-PPh}_2)]$, **2**, and $[Ir_4Pt(dppe)(CO)_9\{\mu\text{-PC(H)Bu}^t\}(\mu\text{-PPh}_2)]$, **3**, on the basis of multinuclear NMR and mass spectrometric studies discussed below, and the structures proposed are shown in Scheme 1. The two other products, $[HIr_4Pt(dppe)(\mu\text{-CO})(CO)_7(\mu\text{-PCH}_2\text{Bu}^t)(\mu\text{-PPh}_2)]$, **4** (red, 5%), and $[Ir_4Pt(dppe)(\mu\text{-CO})(CO)_8(\mu_5\text{-P})(\mu\text{-PPh}_2)]$, **5** (brown, 30%), were fully characterized by spectroscopic data and X-ray analyses.

Characterization of 2 and 3. The $^{31}P\{^1H\}$ NMR spectrum of the mixture containing **2** and **3** showed two sets of four signals [Figure 1a], and a summary of the data is given in Table 1. The ^1H NMR spectrum of this mixture showed no hydride resonance down to −90 °C but exhibited the expected singlets at δ 0.5 and 1.3 (1:1) of the Bu^t, multiplets due the C_6H_5 and CH_2 (of dppe) protons, [Figure 1b]. Resonances at δ 4.2 (dd, $J_{H-P1} = 12$ and $J_{H-P3} = 3$ Hz) and 5.2 (d, $J_{H-P4} \approx 3$ Hz) were shown by $^{31}P-^1H$ HETCOR (Figure 1) to be due to the protons of the coordinated phosphaalkenyl PC(H)Bu^t fragments of compounds **2** and **3**, respectively, formed by hydride transfer to the phosphaalkyne. This experiment also allowed the assignment of all the phosphorus atoms. The NOE difference experiments resulting from

Table 2. Crystal Data and Details of Measurements for Compound 4

Crystal Data	
empirical formula	$C_{51}H_{46}P_4O_8PtIr_4\cdot CH_2Cl_2\cdot{}^1/_2C_6H_{14}$
fw	2002.7
cryst syst	monoclinic
space group	$P2_1/c$ (No. 14)
a (Å)	21.443(7)
b (Å)	12.000(2)
c (Å)	23.469(5)
α (deg)	90
β (deg)	91.22(2)
γ (deg)	90
volume Å^3	6038(3)
Z	4
density (calcd) (Mg/m^3)	2.20
abs coeff (mm^{-1})	11.34
F(000)	3716
cryst size (mm)	0.3 × 0.1 × 0.1 (cut from a needle)
Data Collection	
wavelength (Å)	0.710 73
temp (K)	293(2)
θ range (deg)	2−20
index ranges	$0 \le h \le 20$, $0 \le k \le 11$, $-22 \le l \le 22$
Solution and Refinement	
no. of reflns collected	5818
no. of independent reflns	5630 [R(int) = 0.0428]
no. of reflns with $I > 2\sigma(I)$	3414
structure solution	direct methods
refinement method	full-matrix least-squares on all F^2
no. of data/restraints/params	5630/2/352
goodness-of-fit on F^2	1.071
final R indices [$I > 2\sigma(I)$]	R1 = 0.065, wR2 = 0.141
R indices (all data)	R1 = 0.121, wR2 = 0.173
largest diff peak and hole (e Å^{-3})	1.87 and −1.46 (near Ir and Pt)
abs corr from psi scans	$T_{max} = 1.00$, $T_{min} = 0.74$
maximum shift/esd	0.009

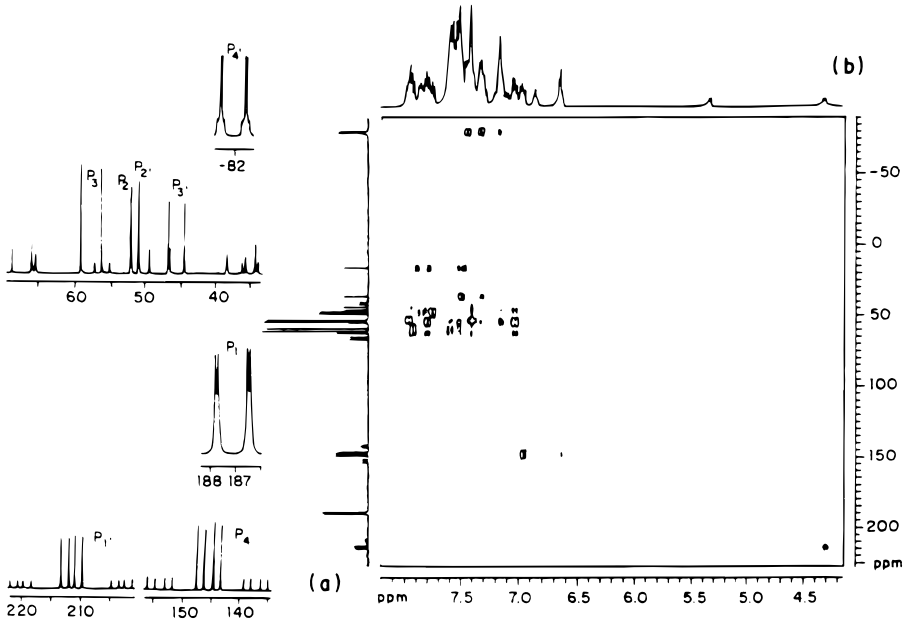

Figure 1. $^{31}P-^{1}H$ heteronuclear correlation spectrum of compounds **2** and **3** in $CDCl_3$ at 25 °C: (a) $^{31}P\{^{1}H\}$ NMR spectrum of **2** and **3**; (b) ^{1}H NMR spectrum of **2** and **3**.

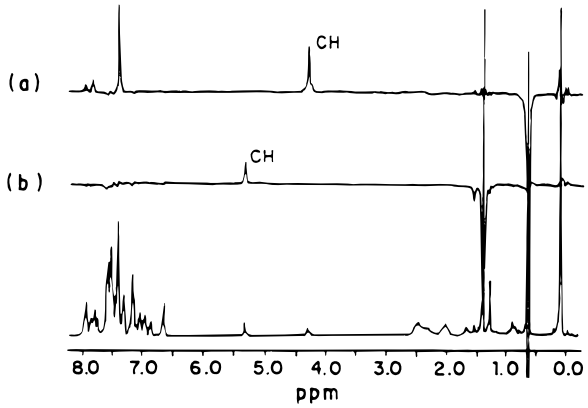

Figure 2. NOE difference spectrum of compounds **2** and **3** in $CDCl_3$ at 25 °C resulting from (a) irradiation of Bu^t at δ 0.5 and (b) irradiation of Bu^t at δ 1.3.

continuous irradiation of the Bu^t resonance at δ 0.5, of compound **2**, showed a space interaction of this group with the CH proton and some of the C_6H_5 protons of the dppe ligand [Figure 2a]. Furthermore, irradiation of the Bu^t resonance at δ 1.3, which is from compound **3**, showed a space interaction only with the CH proton, indicating that there is no phenyl groups next to the Bu^t protons [Figure 2b]. A ^{13}C DEPT (pulse of $\theta = \pi/2$) experiment established that the resonances at δ 37.5 and 38.9 were due to CH carbons of compounds **2** and **3**. The $^{31}P\{^{1}H\}$ NMR spectrum indicated that the PC(H)Bu^t fragment in **2** is bonded to the Pt atom, on the basis of the large value of $^{1}J_{P1'-Pt}$ (2086 Hz), and to one of the Ir atoms that is also bonded to the μ-PPh_2 ligand ($^{2}J_{P1'-P4'} = 161$ Hz). The phosphido P4′ resonance at δ −81.8 in cluster **2** is characteristic of the μ-PPh_2 ligand spanning two iridium atoms that do not interact.[15,16]

The NMR data suggest for compound **3** a structure very similar to that of compound **2**. No coupling between the phosphorus atom P1 of the fragment PC(H)Bu^t and the Pt nucleus was observed in the $^{31}P\{^{1}H\}$ NMR spectrum of compound **3** [Figure 1a], which rules out any direct bond between these two atoms. The

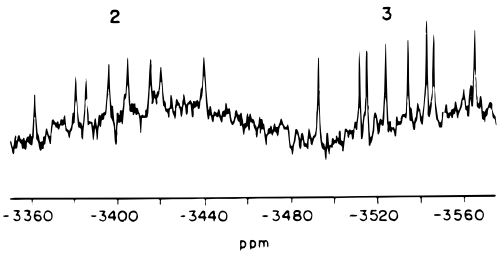

Figure 3. $^{195}Pt\{^{1}H\}$ NMR spectrum of compounds **2** and **3** in CD_2Cl_2 at 25 °C.

phosphido P4 resonance at δ 154.4 for compound **3**, shifted to high frequency in comparison with **2**, suggests the presence of a phosphido group bridging an Ir and a Pt atom that interact.[15,16]

The $^{195}Pt\{^{1}H\}$ NMR spectrum of the mixture of **2** and **3** (δ 1126 and 992, respectively) indicated that the Pt nuclei in the two compounds have very similar environments, as suggested in Figure 3.[17]

Electrospray mass spectra (ESMS) of compounds **2** and **3** gave better results in MeOH with a drop of F_3CCOOH using a low cone angle (20 V) that generated the $[M + H]^+$ species. Two peaks are found in the mass range *m*/*z* 1600−2200, at *m*/*z* 1931 (100) for **2** and *m*/*z* 1903 (45) for **3**. No conclusion about the relative amount of 1931/1903 species can be drawn from the MS results because the intensities reflect the ease of ionization rather than abundances. CO loss can be induced in ESMS by increasing the voltage between the skimmer cones,[18] and with a cone angle of 50 V, a strong peak was observed at *m*/*z* 1874, which could result from the loss of either 2 CO's from compound **2** or 1 CO ligand from compound **3**.

(15) Carty, A. J.; MacLaughlin, S. A.; Nucciarone, D. In *Phosphorus-31 NMR Spectroscopy in Stereochemical Analysis*; Verkade, J. G., Quin, L. D., Eds.; VCH: Weinheim, 1987; pp 559−619.
(16) Benvenutti, M. H. A.; Vargas, M. D.; Braga, D.; Grepioni, F.; Naylor, S.; Mann, B. E. *Organometallics* **1993**, *12*, 2947.
(17) Pregosin, P. S. *Coord. Chem. Rev.* **1982**, *4*, 4247.
(18) Henderson, W.; McIndoe, J. S.; Nicholson, B. K.; Dyson, P. J. *Chem. Commun.* **1996**, 1183.

The variable-temperature $^{13}C\{^1H\}$ NMR experiments (25 to −90 °C) of a ^{13}CO-enriched sample of **2** and **3** in CH_2Cl_2 were used to pinpoint the 19 CO groups, confirming the ESMS results. Furthermore, both the ^{13}C NMR and the solution IR data indicated that compounds **2** and **3** bear only terminally bonded CO ligands in solution.

The metal arrangements proposed for compounds **2** and **3** (see Scheme 1) consist of a Pt edge-bridged Ir_4 butterfly and a Pt edge-bridged Ir_4 tetrahedron, respectively. The μ-PPh_2 and μ-P═CHBu^t ligands were placed on the structures on the basis of the NMR data discussed above and formally contribute each with three electrons. A similar structure containing same Pt(dppe) and a vinylidene fragment was previously established for $[HRu_3Pt(dppe)(CO)_9(\mu_4\text{-}\eta^2\text{-}CC(H)Bu^t)]^+$.[19] Possible structures for compounds **2** and **3** contain 10 and 9 terminal CO ligands, respectively, whose distribution over the metal polyhedra lead to structures in which two Ir and the Pt atoms obey the 18-electron rule and two Ir atoms do not, and contain 19 and 17 electrons. Both structures derive, formally, from a 72-electron trigonal bipyramid with the loss of two and one M−M bonds, respectively. It is interesting that the only 72-electron trigonal bipyramidal $PtIr_4$ cluster reported in the literature, $[PtIr_4(CO)_{12}]^{2-}$, undergoes reversible nucleophilic addition of two CO ligands to give the 76-electron compound $[PtIr_4(CO)_{14}]^{2-}$, with a concomitant elongation of the trigonal bipyramid, instead of M−M bond cleavage.[20]

Characterization of 4. The ^1H NMR spectrum exhibits three sets of multiplets due to the CH_2 groups, a singlet at δ 0.7 for the Bu^t, a multiplet due to the hydride at δ −16.6, and the multiplet due to the Ph protons. With a $^1H-^1H$ COSY experiment it was possible to identify the two different hydrogen atoms of the CH_2 group at δ 0.8 and 1.9 in the $P(CH_2)Bu^t$ fragment. The NOE difference experiments with irradiation of the Bu^t group show the enhancement of those CH_2 protons and of some of the protons of the Ph groups bonded to P2, thus indicating space interaction between these protons.

The $^{13}C\{^1H\}$ NMR spectrum exhibits eight signals due to the carbonyl groups, and it is possible to assign the bridging CO at δ 221.7, which is shifted to high frequency, in comparison with the remaining seven terminal carbonyls. A ^{13}C NMR DEPT (pulse of $\theta = 3\pi/4$) experiment was important to assign the CH_2 groups of the $P(CH_2Bu^t)$ ligand at δ 51.4 and dppe at δ 30.6 and 33.3 and also helped to identify the quaternary carbons in the $^{13}C\{^1H\}$ NMR spectrum. The $^{31}P\{^1H\}$ NMR spectrum of **4** showed four sets of signals (Figure 2), and a summary of the data is given in Table 1. The remarkable low values of the J_{P2-Pt} 153 and J_{P3-Pt} 181 Hz will be discussed later.

Red crystals, suitable for an X-ray diffraction analysis of compound **4**, were obtained by slow evaporation of CH_2Cl_2/hexane from a very concentrated solution. The molecular structure of **4** with the atom-numbering scheme is shown in Figure 4. Crystallographic data are compiled in Table 2, and selected bond distances (Å) and angles (deg) are presented in Table 3. The molecular structure can be described as a square-based pyramidal arrangement of metal atoms with the Ir_3Pt square face capped by a μ_4-PCH_2Bu^t fragment. This structure is similar to that of several other phosphinidene pentanuclear 74 valence electron clusters;[21] however, it is the first example containing a $[Pt(PR_3)_2]$ fragment. The longest and shortest edges of the metal polyhedron (Pt−Ir(3) 2.925(2); Pt−Ir(1) 2.719(2) Å) are spanned by a hydride and an asymmetric CO ligand, respectively, (Ir(1)−C(1) 2.08(3); Pt−C(1) 1.86(3) Å). A third edge [Ir(2)−Ir(4) 2.774(2) Å] is bridged symmetrically by the phosphido group (Ir(2)−P(4) 2.298(9); Ir(4)−P(4) 2.302(8) Å). Of the seven terminal CO ligands, one is bonded to Ir(1) and two are bonded to each of the other iridium atoms. The average Ir−P(1) distance (2.369(9) Å) is comparable to that in the analogous cluster $[Ir_5(CO)_9(\eta^5\text{-}C_5H_5)(\mu_4\text{-}PPh)]$ (2.370(5) Å).[21] The hydride ligand was not located. A space-filling diagram allowed the identification of the hydride position, as a free coordination site seems to be available between the Ir(3) and

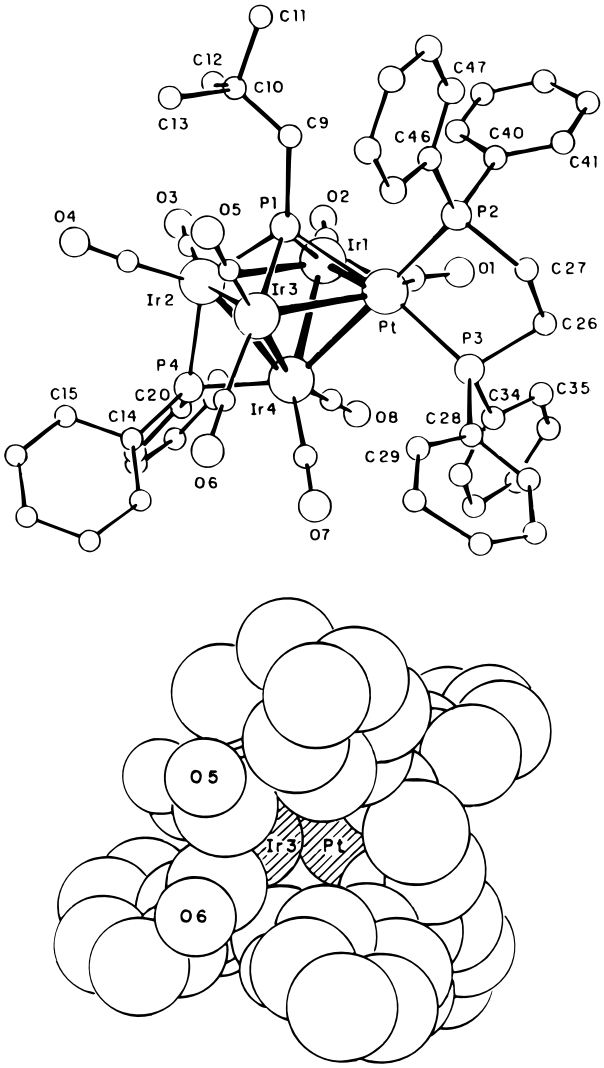

Figure 4. Molecular structure of $[HIr_4Pt(dppe)(\mu\text{-}CO)(CO)_7(\mu\text{-}PCH_2Bu^t)(\mu\text{-}PPh_2)]$ (**4**) and space-filling diagram showing the free coordination site on the edge Ir(3)−Pt.

(19) Ewing, P.; Farrugia, L. J. *Organometallics* **1989**, *8*, 1246.
(20) Fumagalli, A.; Della Pergola, R.; Bonacina, F.; Garlaschelli, L.; Moret, M.; Sironi, A. *J. Am. Chem. Soc.* **1989**, *111*, 165.
(21) Khattar, R.; Naylor, S.; Vargas, M. D.; Braga, D.; Grepioni, F. *Organometallics* **1990**, *9*, 645, and references therein.

Table 3. Selected Bond Distances (Å) and Angles (deg) for $[HIr_4Pt(dppe)(\mu\text{-}CO)(CO)_7(\mu\text{-}PCH_2Bu^t)(\mu\text{-}PPh_2)]$, 4

Pt−C(1)	1.86(3)	Pt−P(2)	2.309(8)	Pt−P(3)	2.315(9)	Pt−P(1)	2.384(9)
Pt−Ir(1)	2.719(2)	Pt−Ir(4)	2.827(2)	Pt−Ir(3)	2.925(2)	Ir(1)−C(2)	1.70(4)
Ir(1)−C(1)	2.08(3)	Ir(1)−P(1)	2.441(9)	Ir(1)−Ir(2)	2.792(2)	Ir(1)−Ir(4)	2.870(2)
Ir(2)−C(4)	1.78(4)	Ir(2)−C(3)	1.82(4)	Ir(2)−P(4)	2.298(9)	Ir(2)−P(1)	2.361(9)
Ir(2)−Ir(4)	2.774(2)	Ir(2)−Ir(3)	2.838(2)	Ir(3)−C(5)	1.72(5)	Ir(3)−C(6)	1.84(4)
Ir(3)−P(1)	2.304(10)	Ir(3)−Ir(4)	2.726(2)	Ir(4)−C(8)	1.77(4)	Ir(4)−C(7)	1.79(4)
Ir(4)−P(4)	2.302(8)	P(1)−C(9)	1.83(4)	P(2)−C(40)	1.81(3)	P(2)−C(27)	1.82(3)
P(2)−C(46)	1.82(4)	P(3)−C(34)	1.78(3)	P(3)−C(26)	1.80(3)	P(3)−C(28)	1.87(3)
P(4)−C(14)	1.77(4)	P(4)−C(20)	1.77(3)	O(1)−C(1)	1.26(3)	O(2)−C(2)	1.22(4)
O(3)−C(3)	1.17(4)	O(4)−C(4)	1.20(4)	O(5)−C(5)	1.22(5)	O(6)−C(6)	1.13(4)
O(7)−C(7)	1.12(4)	O(8)−C(8)	1.20(4)	C(9)−C(10)	1.48(5)	C(26)−C(27)	1.51(4)

C(1)−Pt−P(2)	96.4(10)	P(2)−Pt−P(3)	85.0(3)	P(2)−Pt−P(1)	100.8(3)
P(3)−Pt−P(1)	168.0(3)	C(1)−Pt−Ir(1)	49.7(9)	P(2)−Pt−Ir(1)	122.5(2)
P(3)−Pt−Ir(1)	128.7(2)	P(1)−Pt−Ir(1)	56.7(2)	P(2)−Pt−Ir(4)	172.2(3)
P(3)−Pt−Ir(4)	96.5(2)	P(1)−Pt−Ir(4)	76.4(2)	Ir(1)−Pt−Ir(4)	62.30(5)
C(1)−Pt−Ir(3)	138.7(9)	P(2)−Pt−Ir(3)	116.0(2)	P(3)−Pt−Ir(3)	117.8(2)
P(1)−Pt−Ir(3)	50.2(2)	Ir(1)−Pt−Ir(3)	89.94(6)	Ir(4)−Pt−Ir(3)	56.55(5)
C(2)−Ir(1)−C(1)	106(2)	C(2)−Ir(1)−P(1)	143.3(13)	C(1)−Ir(1)−P(1)	93.4(9)
C(1)−Ir(1)−Pt	43.1(9)	P(1)−Ir(1)−Pt	54.7(2)	P(1)−Ir(1)−Ir(2)	53.1(2)
Pt−Ir(1)−Ir(2)	92.45(6)	P(1)−Ir(1)−Ir(4)	74.8(2)	Pt−Ir(1)−Ir(4)	60.70(5)
Ir(2)−Ir(1)−Ir(4)	58.65(5)	C(4)−Ir(2)−C(3)	102(2)	C(3)−Ir(2)−P(4)	102.4(11)
C(4)−Ir(2)−P(1)	106.3(13)	C(3)−Ir(2)−P(1)	109.8(11)	P(4)−Ir(2)−P(1)	130.1(3)
P(4)−Ir(2)−Ir(4)	53.0(2)	P(1)−Ir(2)−Ir(4)	77.9(2)	P(1)−Ir(2)−Ir(1)	55.8(2)
P(4)−Ir(2)−Ir(1)	100.8(2)	Ir(4)−Ir(2)−Ir(1)	62.09(5)	P(4)−Ir(2)−Ir(3)	90.4(2)
P(1)−Ir(2)−Ir(3)	51.6(3)	Ir(4)−Ir(2)−Ir(3)	58.11(5)	Ir(1)−Ir(2)−Ir(3)	90.30(6)
C(5)−Ir(3)−C(6)	92(2)	C(5)−Ir(3)−P(1)	99(2)	C(5)−Ir(3)−Ir(4)	178(2)
C(6)−Ir(3)−Ir(4)	89.8(12)	P(1)−Ir(3)−Ir(4)	79.8(2)	P(1)−Ir(3)−Ir(2)	53.4(2)
Ir(4)−Ir(3)−Ir(2)	59.76(5)	C(5)−Ir(3)−Pt	120(2)	C(6)−Ir(3)−Pt	127.4(12)
P(1)−Ir(3)−Pt	52.6(2)	Ir(4)−Ir(3)−Pt	59.90(5)	Ir(2)−Ir(3)−Pt	87.32(6)
C(8)−Ir(4)−C(7)	98(2)	C(8)−Ir(4)−P(4)	99.6(11)	C(7)−Ir(4)−P(4)	104.1(12)
C(8)−Ir(4)−Ir(3)	162.5(11)	C(7)−Ir(4)−Ir(3)	90.3(13)	P(4)−Ir(4)−Ir(3)	93.2(2)
P(4)−Ir(4)−Ir(2)	52.8(2)	Ir(3)−Ir(4)−Ir(2)	62.12(5)	P(4)−Ir(4)−Pt	143.3(2)
Ir(3)−Ir(4)−Pt	63.55(5)	Ir(2)−Ir(4)−Pt	90.55(5)	P(4)−Ir(4)−Ir(1)	98.4(3)
Ir(3)−Ir(4)−Ir(1)	90.96(6)	Ir(2)−Ir(4)−Ir(1)	59.27(5)	Pt−Ir(4)−Ir(1)	57.00(5)
C(9)−P(1)−Ir(3)	126.7(13)	C(9)−P(1)−Ir(2)	127.7(13)	Ir(3)−P(1)−Ir(2)	74.9(3)
C(9)−P(1)−Pt	117.1(12)	Ir(3)−P(1)−Pt	77.2(3)	Ir(2)−P(1)−Pt	114.0(3)
C(9)−P(1)−Ir(1)	118.4(13)	Ir(3)−P(1)−Ir(1)	114.5(4)	Ir(2)−P(1)−Ir(1)	71.1(2)
Pt−P(1)−Ir(1)	68.6(2)	C14−P(4)−C20	103(2)	Ir(2)−P(4)−Ir(4)	74.2(3)
C34−P(3)−C28	100.6(14)	C26−P(3)−Pt	106.7(11)	C40−P(2)−C46	104(2)
C(40)−P(2)−Pt	121.5(11)	C(27)−P(2)−Pt	105.0(11)	C(10)−C(9)−P(1)	125(3)
C27−C26−P(3)	107(2)	C26−C27−P(2)	110(2)		

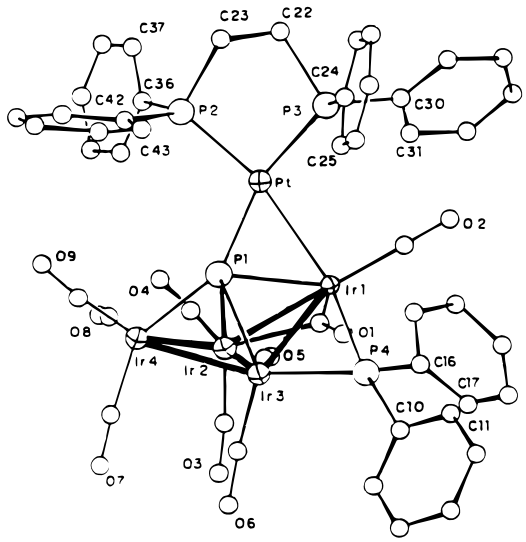

Figure 5. Molecular structure of $[Ir_4Pt(dppe)(\mu\text{-}CO)(CO)_8(\mu_5\text{-}P)(\mu\text{-}PPh_2)]$ (**5**). Selected bond distances (Å): Ir(1)−Ir(2) 2.885(2), Ir(1)−Ir(3) 2.867(2), Ir(2)−Ir(3) 2.724(3), Ir(2)−Ir(4) 2.777(3), Ir(3)−Ir(4) 2.786(2), Pt−Ir(1) 2.751(2).

Pt(1) metal atoms (Figure 4). Selective decoupling of the four phosphorus atoms in a ^1H NMR experiment was used to confirm this assignment.

As expected, the platinum atom in **4** bears the dppe ligand. However, interestingly, although the multinuclear NMR data for compound **4** are in accord with the solid-state structure, the values observed for $^1J_{P2-Pt}$ and $^1J_{P3-Pt}$ (153 and 181 Hz, respectively) are exceptionally low. Similar low values for $^1J_{P-Pt}$ have been reported for the η^2-ligated phosphaalkynes and phosphaalkenes where the s-character of the Pt−P bond is very low.[22] In complex **4** this effect is pronounced, presumably because although the P lone pair electrons involved in the Pt−P bonds are in roughly sp^3 hybrid orbitals, the high participation of the Pt s-orbital in the framework bonding of this unsaturated 74-electron system leaves very little s-character on the Pt hybrid orbitals involved with the dppe ligand. This is in sharp contrast with other tetrahedral, butterfly, and triangular clusters containing $Pt(PR_3)_2$, where values of $^1J_{P-Pt}$ can exceed 5500 Hz.[23]

Characterization of 5. The results obtained from the ^1H NMR spectrum were unexpected, as no resonance for the Bu^t group was present and the only resonances were the phenyl proton multiplets and the multiplets of the CH_2 groups of the dppe ligand. The $^{13}C\{^1H\}$ NMR confirmed this result, as the only reso-

(22) Burckett-St Laurent, J. C. R.; Hitchcock, P. B.; Kroto, H. W.; Nixon, J. F. *J. Chem. Soc., Chem. Commun.* **1981**, 1141.

(23) (a) Davies, D. L.; Jeffrey, J. C.; Miguel, D.; Sherwood, P.; Stone, F. G. A. *J. Chem. Soc., Chem. Commun.* **1987**, 454. (b) Davies, D. L.; Jeffrey, J. C.; Miguel, D.; Sherwood, P.; Stone, F. G. A. *J. Organomet. Chem.* **1990**, *383*, 463. (c) Farrugia, L. J. *Adv. Organomet. Chem.* **1990**, *31*, 301, and references therein.

Table 4. Selected Atomic Coordinates ($\times 10^4$) and Equivalent Isotropic Displacement Parameters ($Å^2 \times 10^3$) for 4

	x	*y*	*z*	*U*(eq)[a]
Pt	2712(1)	1939(1)	2264(1)	39(1)
Ir(1)	3480(1)	1959(1)	1356(1)	42(1)
Ir(2)	2477(1)	1983(1)	577(1)	46(1)
Ir(3)	1627(1)	1961(1)	1487(1)	47(1)
Ir(4)	2503(1)	327(1)	1402(1)	41(1)
P(1)	2516(5)	3028(7)	1429(4)	45(2)
P(2)	2740(5)	3310(7)	2954(3)	43(3)
P(3)	2704(5)	712(7)	3024(4)	45(3)
P(4)	2327(5)	106(8)	438(4)	49(3)
O(1)	4088(11)	1611(18)	2482(9)	56(7)
O(2)	4713(14)	2081(24)	863(12)	95(9)
O(3)	3574(13)	2394(22)	−150(11)	84(8)
O(4)	1535(15)	3052(27)	−190(13)	109(10)
O(5)	728(14)	3815(26)	1514(12)	100(10)
O(6)	611(14)	290(25)	1420(11)	93(9)
O(7)	1699(12)	−1326(22)	1912(10)	73(8)
O(8)	3663(12)	−1001(21)	1543(10)	71(8)
C(1)	3570(15)	1738(26)	2231(12)	43(9)
C(2)	4216(18)	2005(31)	1105(15)	62(11)
C(3)	3169(17)	2256(28)	167(14)	52(10)
C(4)	1879(20)	2589(36)	144(18)	84(13)
C(5)	1087(22)	3023(41)	1521(19)	98(15)
C(6)	1007(19)	906(34)	1425(16)	72(12)
C(7)	1986(19)	−649(35)	1720(16)	73(12)
C(8)	3201(18)	−452(31)	1484(14)	60(11)
C(9)	2571(17)	4541(30)	1505(16)	67(11)
C(10)	2548(18)	5353(32)	1030(16)	67(11)
C(11)	2626(20)	6557(35)	1285(17)	100(15)
C(12)	3008(31)	5235(60)	598(27)	213(32)
C(13)	1902(31)	5404(62)	691(28)	223(34)
C(14)	1603(17)	−417(31)	179(14)	60(10)
C(20)	2881(15)	−667(26)	52(13)	45(9)
C(26)	2915(15)	1506(26)	3652(12)	46(9)
C(27)	2564(16)	2594(27)	3615(14)	55(10)
C(28)	3263(14)	−480(26)	3044(12)	38(8)
C(34)	2015(15)	46(26)	3269(13)	43(9)
C(40)	2205(16)	4480(28)	2928(13)	48(9)
C(46)	3500(18)	3956(30)	3076(16)	65(11)

[a] *U*(eq) is defined as one-third of the trace of the orthogonalized U_{ij} tensor.

nances observed were the aromatic carbons of the C_6H_5 groups and two multiplets for the CH_2 carbons of the dppe ligand. In the $^{31}P\{^1H\}$ NMR spectrum it is possible to distinguish four phosphorus nuclei coupling with each other and with the platinum atom, as shown in Table 1.

The molecular structure of compound **5**, which was established by an X-ray analysis, despite the poor quality of the crystallographic data (Figure 5), consists of a butterfly arrangement of iridium atoms with a semi-interstitial phosphide P(1) interacting with the four atoms of the butterfly. The Pt(dppe) fragment bridges the Ir(1)−P(1) bond; the phosphido group and a CO span two edges of the same wing (Ir(1)−Ir(3) and Ir(1)−Ir(2), respectively), and the other eight CO ligands are distributed in such a way that all iridium atoms obey the 18-electron rule. These results are in agreement with the solution characterization of **5**. To our knowledge, the only other pentanuclear cluster with a partially encapsulated phosphide is $[Ru_5(CO)_{16}(\mu\text{-}PPh_2)(\mu_5\text{-}P)]$, which exhibits an open array of ruthenium atoms different from that of **5**.[24] The structure of **5** can be considered reminiscent of that of the butterfly carbyne cluster $[HFe_4(CO)_{12}(\mu_4\text{-}\eta^2\text{-}CH)]$, with a PPt(dppe) fragment formally replacing CH in the iron cluster.[25]

We can only speculate on the pathway of formation of the phosphaalkenyl-containing clusters **2** and **3**. It seems likely that initial nucleophilic attack at **1** of the coordinated phosphaalkyne via the phosphorus lone pair electrons is followed by migratory insertion into the Ir−H−Ir bond to give a metallaphosphaalkene butterfly complex "$[Ir_4(CO)_{10}(\mu\text{-}PPh_2)\mu\text{-}\{(\eta^2\text{-}PCHBu^t)Pt(dppe)\}]$". Further interaction of the PCHButPt(dppe) fragment, with formation of Pt−Ir bonds and cleavage of an Ir−Ir bond, would lead to the formation of compound **2**, while rearrangements of the PPh_2 and $P{=}CHBu^t$ fragments over the metal frame and CO loss lead to compound **3**. Migration of the μ-PPh_2 in **1** has been observed upon reaction with DBU and $[Rh(CO)_2(MeCN)_2]SbF_6$ that yielded the trigonal bipyramidal compound $[RhIr_4(\mu\text{-}PPh_2)(CO)_{10}]$ with the μ-PPh_2 bridging a Rh−Ir bond.[26]

Acknowledgment. We acknowledge financial support from the Commission of European Communities, CNPq, FAPESP, and PADCT (Brazil). We thank Prof. Brian Nicholson, University of Waikato, Hamilton, New Zealand, for the electrospray mass spectrometry (ESMS) measurements.

Supporting Information Available: Tables of bond distances and bond angles, atomic coordinates, anisotropic displacement coefficients, hydrogen coordinates, and isotropic displacement parameters for **4** and crystal data and details of measurements for **5** (8 pages). Ordering information is given on any current masthead page.

OM980317W

(24) MacLaughlin, S. A.; Taylor, N.; Carty, A. J. *Inorg. Chem.* **1983**, *22*, 1409.
(25) Beno, M. A.; Williams, J. M.; Tachikawa, M.; Muetterties, E. L. *J. Am. Chem. Soc.* **1981**, *103*, 1485.
(26) Braga, D.; Grepioni, F.; Squizani, F.; Vargas, M. D. Unpublished results.